



ELSEVIER

Available online at www.sciencedirect.com

SCIENCE @ DIRECT®

Computers and Mathematics with Applications 48 (2004) 1087–1100

An International Journal
**computers &
mathematics**
with applications

www.elsevier.com/locate/camwa

Characteristic-Nonconforming Finite-Element Methods for Advection-Dominated Diffusion Problems

ZHANGXIN CHEN

Department of Mathematics, Box 750156
Southern Methodist University
Dallas, TX 75275-0156, U.S.A.
zchen@mail.smu.edu

Abstract—In this paper characteristic-nonconforming finite-element methods are studied for time dependent advection-dominated diffusion problems. The diffusion term in these problems is discretized using nonconforming finite elements, and the temporal differentiation and advection terms are treated by characteristic tracking schemes. Various nonconforming finite elements and characteristic tracking schemes are studied. Stability and convergence properties of the characteristic nonconforming methods are obtained; unconditionally stable results and error estimates of optimal order are established. © 2004 Elsevier Ltd. All rights reserved.

Keywords—Characteristics-based methods, Nonconforming finite-element methods, Advection-dominated diffusion problems, Stability, Convergence, Error estimates.

1. INTRODUCTION

In this paper we study an application of the nonconforming finite-element method to the reaction-diffusion-advection problem

$$\frac{\partial(cp)}{\partial t} + \nabla \cdot (\mathbf{b}p - \mathbf{a}\nabla p) + Rp = f, \quad (1.1)$$

for the unknown solution p , where c , \mathbf{b} (vector), \mathbf{a} (tensor), R , and f are given functions. Note that (1.1) involves advection (\mathbf{b}), diffusion (\mathbf{a}), and reaction (R). Many problems arise in this form, e.g., transport problems for multiphase flow in porous media and density problems for semiconductor modeling. When diffusion dominates advection, the standard finite-element method performs well for (1.1). When advection dominates diffusion, however, it does not work well. In particular, it exhibits excessive nonphysical oscillations when the solution to (1.1) is not smooth. Standard upstream weighting approaches have been applied to the finite-element method with the purpose of eliminating the nonphysical oscillations, but these approaches smear sharp fronts of the solution and suffer from grid-orientation difficulties. Although extremely fine mesh refinement is possible to overcome some of these difficulties, it is not efficient due to the excessive computational effort.

This work is supported in part by National Science Foundation Grants DMS-9972147 and INT-9901498.

Many numerical methods have been developed for solving (1.1) where advection dominates, such as the optimal spatial method. This method employs an Eulerian approach that is based on the minimization of the error in the approximation of spatial derivatives and the use of optimal test functions satisfying a local adjoint problem [1,2]. It yields an upstream bias in the resulting approximation and have the features:

- (a) time truncation errors dominate the solution;
- (b) the solution has significant numerical diffusion and phase errors;
- (c) the Courant number is generally restricted to be less than one.

Other Eulerian methods such as the Petrov-Galerkin finite-element method have been developed to use nonzero spatial truncation errors to cancel temporal errors and thereby reduce the overall truncation errors [3,4]. While these methods improve accuracy in the approximation of the solution, they still suffer from a strict Courant number limitation.

Another class of numerical methods for the solution of (1.1) are the Eulerian-Lagrangian methods. Because of the Lagrangian nature of advection, these methods treat the advection by a characteristic tracking approach. They have shown great potential. The common features of this class are:

- (a) the Courant number restriction of the purely Eulerian methods is alleviated because of the Lagrangian nature of the advection step;
- (b) since the spatial and temporal dimensions are coupled through the characteristic tracking, the effect of time truncation errors present in optimal spatial methods is greatly reduced;
- (c) they produce nonoscillatory solutions without numerical diffusion, using reasonably large time steps on grids no finer than necessary to resolve the solution on the moving fronts.

The Eulerian-Lagrangian methods have been applied in the context of the standard conforming and mixed finite-element methods [5–8]. In this paper we extend these methods to the setting of the nonconforming finite-element method. The reasons for the wide use of the nonconforming method in fluid and solid mechanics are that they involve fewer degrees of freedom (particularly for partial differential equations of order higher than two) and the coefficient matrices of linear systems arising from this method are better conditioned when an appropriate set of basis functions of finite-element spaces are used.

2. MMOC-NONCONFORMING FINITE-ELEMENT METHODS

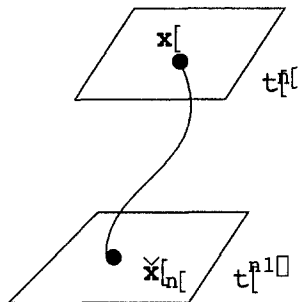
2.1. The Continuous Problem

To see the idea of combining a characteristic method and the nonconforming finite-element method, we first consider the modified method of characteristics (MMOC) [8,9]. The MMOC is simple to set up and analyze, and is still in wide use. It is based on the nondivergence form of (1.1)

$$c(\mathbf{x}) \frac{\partial p}{\partial t} + \mathbf{b}(\mathbf{x}, t) \cdot \nabla p - \nabla \cdot (\mathbf{a}(\mathbf{x}, t) \nabla p) + R(\mathbf{x}, t)p = f(\mathbf{x}, t), \quad \mathbf{x} \in \Omega, \quad t > 0, \quad (2.1)$$

where $\Omega \subset \mathbb{R}^d$ ($d \leq 3$) is a bounded domain with boundary Γ . To complete this equation, we need boundary and initial conditions. It is well known that the MMOC is not so flexible in the treatment of general boundary conditions. Thus, to avoid the difficulty associated with the boundary conditions, we assume that (2.1) is Ω -periodic; i.e., Ω is a rectangle (respectively, a rectangular parallelepiped), and all functions in (2.1) are spatially Ω -periodic. In fact, this is physically reasonable because no-flow boundaries are usually handled by reflection and interior flow behavior is often much more important than boundary effects in fluid flow problems, for example. The treatment of other boundary conditions will be considered in the fourth section where an Eulerian-Lagrangian approach is adopted. The initial condition is

$$p(\mathbf{x}, 0) = p_0(\mathbf{x}), \quad \mathbf{x} \in \Omega. \quad (2.2)$$

Figure 1. An illustration of the definition \check{x}_n .

Let

$$\psi(\mathbf{x}, t) = (c^2(\mathbf{x}) + |\mathbf{b}(\mathbf{x}, t)|^2)^{1/2},$$

where $|\mathbf{b}|^2 = b_1^2 + b_2^2 + \dots + b_d^2$, with $\mathbf{b} = (b_1, b_2, \dots, b_d)$, $d \leq 3$. Throughout this paper, assume that

$$c(\mathbf{x}) > 0, \quad \mathbf{x} \in \Omega. \quad (2.3)$$

Let the characteristic direction corresponding to the hyperbolic part of (2.1), $c \frac{\partial p}{\partial t} + \mathbf{b} \cdot \nabla p$, be denoted by τ , so

$$\frac{\partial}{\partial \tau} = \frac{c(\mathbf{x})}{\psi(\mathbf{x}, t)} \frac{\partial}{\partial t} + \frac{1}{\psi(\mathbf{x}, t)} \mathbf{b}(\mathbf{x}, t) \cdot \nabla.$$

With this definition, equation (2.1) becomes

$$\psi(\mathbf{x}, t) \frac{\partial p}{\partial \tau} - \nabla \cdot (\mathbf{a}(\mathbf{x}, t) \nabla p) + R(\mathbf{x}, t)p = f(\mathbf{x}, t), \quad \mathbf{x} \in \Omega, \quad t > 0. \quad (2.4)$$

For $k \geq 0$, the standard Sobolev spaces $H^k(\Omega) = W^{k,2}(\Omega)$ are used in this paper, with the usual norms. For $k = 0$, set $L^2(\Omega) = H^0(\Omega)$. In addition, we define the linear space

$$V = \{v \in H^1(\Omega) : v \text{ is } \Omega\text{-periodic}\}.$$

We also define the inner product in $L^2(\Omega)$

$$(v, w)_S = \int_S v(\mathbf{x}) w(\mathbf{x}) d\mathbf{x}.$$

If $S = \Omega$, we omit it in this notation. Now, applying Green's formula in space and the periodic boundary condition, (2.2) and (2.4) are written in the equivalent variational form

$$\begin{aligned} \left(\psi \frac{\partial p}{\partial \tau}, v \right) + (\mathbf{a} \nabla p, \nabla v) + (Rp, v) &= (f, v), \quad v \in V, \quad t > 0, \\ p(\mathbf{x}, 0) &= p_0(\mathbf{x}), \quad \mathbf{x} \in \Omega. \end{aligned} \quad (2.5)$$

2.2 MMOC-Nonconforming Methods

Let $0 = t^0 < t^1 < \dots < t^n < \dots$ be a partition in time, with $\Delta t^n = t^n - t^{n-1}$. For a generic function v , set $v^n = v(t^n)$. A characteristic is approximated by

$$\check{x}_n = \mathbf{x} - \frac{\Delta t^n}{c(\mathbf{x})} \mathbf{b}(\mathbf{x}, t^n). \quad (2.6)$$

Furthermore, we see that, at $t = t^n$,

$$\begin{aligned} \psi \frac{\partial p}{\partial \tau} &\approx \psi(\mathbf{x}, t^n) \frac{p(\mathbf{x}, t^n) - p(\check{x}_n, t^{n-1})}{(|\mathbf{x} - \check{x}_n|^2 + (\Delta t^n)^2)^{1/2}} \\ &= c(\mathbf{x}) \frac{p(\mathbf{x}, t^n) - p(\check{x}_n, t^{n-1})}{\Delta t^n}. \end{aligned} \quad (2.7)$$

That is, a backtracking algorithm is used to approximate the characteristic derivative (see Figure 1).

Let K_h be a regular triangulation of Ω into nonoverlapping (open) finite elements K ,

$$\bar{\Omega} = \bigcup_{K \in K_h} \bar{K},$$

such that no vertex of one element lies on an edge (or face) of another element, where $\bar{\Omega}$ and \bar{K} represent the closure of Ω and K (i.e., $\bar{\Omega} = \Omega \cup \Gamma$ and $\bar{K} = K \cup \partial K$), respectively. The mesh parameters h_K and h are defined as follows:

$$h_K = \text{diam}(K) \quad \text{and} \quad h = \max_{K \in K_h} h_K,$$

where $\text{diam}(K)$ is the length of the longest edge of \bar{K} . Associated with K_h , let V_h be a nonconforming finite-element space. Examples will be given later.

The MMOC for (2.1) is given: for $n = 1, 2, \dots$, find $p_h^n \in V_h$ such that

$$\left(c \frac{p_h^n - \tilde{p}_h^{n-1}}{\Delta t^n}, v \right) + \sum_{K \in K_h} (a^n \nabla p_h^n, \nabla v)_K + (R^n p_h^n, v) = (f^n, v), \quad \forall v \in V_h, \quad (2.8)$$

where

$$\tilde{p}_h^{n-1} = p_h(\tilde{\mathbf{x}}_n, t^{n-1}) = p_h\left(\mathbf{x} - \frac{\Delta t^n}{c(\mathbf{x})} \mathbf{b}(\mathbf{x}, t^n), t^{n-1}\right). \quad (2.9)$$

The initial approximation p_h^0 can be defined as any reasonable approximation of p_0 in V_h ; see (5.4) later.

In addition to assumption (2.3), we assume that the coefficients a_{ij} , b_i , c , and R are bounded in Ω ,

$$0 \leq R(\mathbf{x}, t), \quad a_* \sum_{i=1}^d y_i^2 \leq \sum_{i,j=1}^d a_{ij}(\mathbf{x}, t) y_i y_j, \quad \forall \mathbf{y} \in \mathbb{R}^d, \quad \mathbf{x} \in \Omega, \quad t > 0, \quad (2.10)$$

and

$$c \in W^{1,\infty}(\Omega), \quad bc \in (L^\infty(J; W^{1,\infty}(\Omega)))^d, \quad (2.11)$$

where $a_* > 0$ is a real number and $J = (0, T]$ ($T > 0$).

Existence and uniqueness of a solution to problem (2.8) can be easily checked. In fact, since it is a finite-dimensional system, it suffices to show uniqueness. Setting $f \equiv 0$ and choosing $v = p_h^n$ in (2.8), we see that

$$(cp_h^n, p_h^n) + \sum_{K \in K_h} (a^n \nabla p_h^n, \nabla p_h^n)_K \Delta t^n + (R^n p_h^n, p_h^n) \Delta t^n = (c\tilde{p}_h^{n-1}, p_h^n),$$

so that, by (2.3), (2.10), and an induction argument (also setting $p_h^0 = 0$),

$$p_h^n(\mathbf{x}) = 0, \quad \mathbf{x} \in \Omega.$$

THEOREM 2.1. *Under (2.3) and (2.10), system (2.8) has a unique solution. Furthermore, if (2.11) holds, so does the stability result*

$$\|p_h\|_{L^\infty(J; L^2(\Omega))} + \left(\sum_{K \in K_h} \|\nabla p_h\|_{L^2(K \times J)}^2 \right)^{1/2} \leq C (\|f\|_{L^2(\Omega_T)} + \|p_0\|_{L^2(\Omega)}), \quad (2.12)$$

where $\Omega_T = \Omega \times J$ and the constant C is independent of h .

This stability result will be proven in the fifth section.

2.3. Examples

In this section we give some examples of the nonconforming finite-element space V_h where the periodic boundary condition is implicitly imposed.

2.3.1. The Crouzeix-Raviart element

Let K_h be a triangulation of $\Omega \subset \mathbb{R}^2$ into triangles $\{K\}$, and define [10]

$$V_h = \left\{ v \in L^2(\Omega) : v|_K \text{ is linear, } K \in K_h, \text{ and } v \text{ is continuous} \right. \\ \left. \text{at the midpoints of interior edges} \right\}.$$

This is the simplest nonconforming finite element for second-order partial differential equations. Set

$$\Delta t = \max_{n=1,2,\dots} \Delta t^n.$$

THEOREM 2.2. *Under (2.3), (2.10), and (2.11) and with an appropriate choice of p_h^0 , if p and p_h are the respective solutions of (2.5) and (2.8), for Δt sufficiently small, we have*

$$\left(\sum_{n=1}^N \sum_{K \in K_h} \|p^n - p_h^n\|_{H^1(K)}^2 \Delta t^n \right)^{1/2} \leq C \left\{ \Delta t \left\| \frac{\partial^2 p}{\partial \tau^2} \right\|_{L^2(\Omega_T)} \right. \\ \left. + h \left(\|p\|_{L^\infty(J; H^2(\Omega))} + \left\| \frac{\partial p}{\partial t} \right\|_{L^2(J; H^1(\Omega))} \right) \right\}, \quad (2.13)$$

where the constant C is independent of h and N is such that $\Delta t^N = T$.

The proof of Theorem 2.2 will be also given in the fifth section. More estimates for the error $p - p_h$ in other norms will be obtained in a forthcoming paper.

It is obvious that the linear system arising from (2.8) is symmetric and positive definite under (2.10), even in the presence of the advection term. With the usual choice of basis functions in V_h , this system has a condition number of order

$$\mathcal{O} \left(1 + \max_{\mathbf{x} \in \Omega, t \geq 0, i, j=1, \dots, d} |a_{ij}(\mathbf{x}, t)| h^{-2} \Delta t \right). \quad (2.14)$$

Furthermore, if a hierarchical basis on multigrids is constructed for V_h [11], the condition number can be improved to

$$\mathcal{O} \left(1 + \max_{\mathbf{x} \in \Omega, t \geq 0, i, j=1, \dots, d} |a_{ij}(\mathbf{x}, t)| h^{-1} \Delta t \right). \quad (2.15)$$

Therefore, we see that when $\Delta t = \mathcal{O}(h)$, a conjugate gradient algorithm applied to the solution of the linear system arising from (2.8) is optimal in the sense that the iteration number is independent of h .

2.3.2. The rotated Q_1 element

Let K_h be a partition of Ω into rectangles $\{K\}$ such that the horizontal and vertical edges of rectangles are parallel to the x_1 - and x_2 -coordinate axes, respectively, and adjacent elements completely share their common edge. Associated with K_h , we define the nonconforming finite-element space on rectangles

$$V_h = \left\{ v \in L^2(\Omega) : v|_K = a_K^1 + a_K^2 x_1 + a_K^3 x_2 + a_K^4 (x_1^2 - x_2^2), \right. \\ \left. a_K^i \in \mathbb{R}, K \in K_h, \text{ and } v \text{ is continuous at the} \right. \\ \left. \text{midpoints of interior edges} \right\}.$$

This rectangular nonconforming element is termed the *rotated Q_1 element* [12,13] because of the fact that $x_1^2 - x_2^2$ can be generated from $x_1 x_2$ by a rotation of 45° . The degrees of freedom for this element can be chosen in a different way,

$$V_h = \left\{ v \in L^2(\Omega) : v|_K = a_K^1 + a_K^2 x_1 + a_K^3 x_2 + a_K^4 (x_1^2 - x_2^2), \right. \\ \left. a_K^i \in \mathbb{R}, K \in K_h, \text{ and if } K_1 \text{ and } K_2 \text{ share an} \right. \\ \left. \text{edge } e, \text{ then } \int_e v|_{\partial K_1} d\ell = \int_e v|_{\partial K_2} d\ell \right\}.$$

Theorems 2.1 and 2.2 and estimate (2.14) hold for the rotated Q_1 element as well. Moreover, if a hierarchical basis on multilevel grids is constructed for this element [14], (2.15) is also true.

The rotated Q_1 nonconforming element is the simplest available on rectangles. The next simplest element is the Wilson nonconforming element [15], which has the same error estimates as this Q_1 element, but has more degrees of freedom. Hence, we will not discuss the Wilson element.

2.3.3. A nonconforming element on tetrahedra

Let K_h be a partition of $\Omega \subset \mathbb{R}^3$ into tetrahedra $\{K\}$ such that adjacent elements completely share their common face. The following space is the three-dimensional analogue of the Crouzeix-Raviart space on triangles [16]:

$$V_h = \left\{ v \in L^2(\Omega) : v|_K \in P_1(K), K \in K_h, \text{ and } v \text{ is continuous} \right. \\ \left. \text{at the centroids of interior faces} \right\}.$$

Theorems 2.1 and 2.2 and estimate (2.14) hold for this and next two three-dimensional nonconforming elements. But estimate (2.15) has not been shown yet.

2.3.4. A nonconforming element on rectangular parallelepipeds

Let K_h be a partition of Ω into rectangular parallelepipeds $\{K\}$ such that their faces are parallel to the coordinate axes and adjacent elements completely share their common face. As in the two-dimensional case, the rotated Q_1 nonconforming element in three dimensions can be defined using two different sets of degrees of freedom. Namely, it can be defined either in terms of nodal values [16]

$$V_h = \left\{ v \in L^2(\Omega) : v|_K = a_K^1 + a_K^2 x_1 + a_K^3 x_2 + a_K^4 x_3 + a_K^5 (x_1^2 - x_2^2) \right. \\ \left. + a_K^6 (x_1^2 - x_3^2), a_K^i \in \mathbb{R}, K \in K_h, \text{ and } v \text{ is} \right. \\ \left. \text{continuous at the centroids of interior faces} \right\},$$

or in terms of integrals over faces

$$V_h = \left\{ v \in L^2(\Omega) : v|_K = a_K^1 + a_K^2 x_1 + a_K^3 x_2 + a_K^4 x_3 + a_K^5 (x_1^2 - x_2^2) \right. \\ \left. + a_K^6 (x_1^2 - x_3^2), a_K^i \in \mathbb{R}, K \in K_h, \text{ and if } K_1 \text{ and } K_2 \right. \\ \left. \text{share a face } e, \text{ then } \int_e v|_{\partial K_1} d\ell = \int_e v|_{\partial K_2} d\ell \right\}.$$

Again, they produce the same convergence rate as in Theorem 2.2, but the second definition seems to yield a better conditioned stiffness system [14].

2.3.5. A nonconforming element on prisms

Let K_h be a partition of Ω into prisms $\{K\}$ such that their base is a triangle in the (x_1, x_2) -plane with three vertical edges parallel to the x_3 -axis and adjacent prisms completely share their common face. The nonconforming finite elements on prisms are analogues of those on rectangular parallelepipeds. Hence they can be defined using two different sets of degrees of freedom. As an example, we present them in terms of the integrals over faces [16],

$$V_h = \left\{ v \in L^2(\Omega) : v|_K = a_K^1 + a_K^2 x_1 + a_K^3 x_2 + a_K^4 x_3 + a_K^5 (x_1^2 + x_2^2 - 2x_3^2), \right. \\ \left. a_K^i \in \mathbb{R}, K \in K_h, \text{ and if } K_1 \text{ and } K_2 \right. \\ \left. \text{share a face } e, \text{ then } \int_e v|_{\partial K_1} d\ell = \int_e v|_{\partial K_2} d\ell \right\}.$$

3. MMOCAA-NONCONFORMING FINITE-ELEMENT METHODS

Problem (2.1) with the periodic boundary condition is considered in this section. Furthermore, to introduce the methods, we assume in this section that

$$\nabla \cdot \mathbf{b} = 0, \quad \text{in } \Omega, \quad t > 0. \quad (3.1)$$

That is, \mathbf{b} is divergence-free. This is physically reasonable since \mathbf{b} is typically a velocity field and (3.1) corresponds to the incompressibility condition. Note that, by (3.1), the periodicity assumption, and the divergence theorem, equation (2.1) with $R = 0$ and $f = 0$ yields the conservation law

$$\int_{\Omega} c(\mathbf{x}) p(\mathbf{x}, t) d\mathbf{x} = \int_{\Omega} c(\mathbf{x}) p^0(\mathbf{x}) d\mathbf{x}, \quad t > 0. \quad (3.2)$$

In real applications, it is desirable to maintain at least a discrete form of this law in any numerical approximation of (2.1). However, in general, (2.8) does not satisfy this property, and it creates an imbalance in mass. The imbalance stems from the advection (transport) process since the diffusion process in (2.8) has been shown to conserve mass locally [8]. To see this, set $\mathbf{a} = \mathbf{0}$, $R = f = 0$, and $v = 1$ in (2.8) to have

$$\int_{\Omega} c(\mathbf{x}) p_h^n(\mathbf{x}) d\mathbf{x} = \int_{\Omega} c(\mathbf{x}) \tilde{p}_h^{n-1}(\mathbf{x}) d\mathbf{x} \neq \int_{\Omega} c(\mathbf{x}) p_h^{n-1}(\mathbf{x}) d\mathbf{x}. \quad (3.3)$$

Note that in the case where c is constant, preserving (3.2) requires that the Jacobian of the map (2.6) identically equal one. However, in general, if $\nabla \cdot (\mathbf{b}/c) \neq 0$, the Jacobian is $1 + O(\Delta t)$, and it is $1 + O((\Delta t)^2)$ if (3.1) holds and c is constant. To preserve (3.2) numerically, we follow [17] to use the modified method of characteristics with adjusted advection (MMOCAA).

Let V_h and p_h^0 be defined as in the previous section. For $1 \leq n \leq N$, given $p_h^{n-1} \in V_h$, set

$$Q_h^{n-1} = \int_{\Omega} c(\mathbf{x}) p_h^{n-1}(\mathbf{x}) d\mathbf{x}, \quad \tilde{Q}_h^{n-1} = \int_{\Omega} c(\mathbf{x}) \tilde{p}_h^{n-1}(\mathbf{x}) d\mathbf{x}.$$

As mentioned above, $Q_h^{n-1} \neq \tilde{Q}_h^{n-1}$ in general. Define

$$\tilde{p}_h^{n-1}(\mathbf{x}) = \begin{cases} \max \{ p_h^{n-1}(\tilde{\mathbf{x}}^-), p_h^{n-1}(\tilde{\mathbf{x}}^+) \}, & \text{if } \tilde{Q}_h^{n-1} < Q_h^{n-1}, \\ \min \{ p_h^{n-1}(\tilde{\mathbf{x}}^-), p_h^{n-1}(\tilde{\mathbf{x}}^+) \}, & \text{if } \tilde{Q}_h^{n-1} > Q_h^{n-1}, \end{cases}$$

and

$$\tilde{Q}_h^{n-1} = \int_{\Omega} c(\mathbf{x}) \tilde{p}_h^{n-1}(\mathbf{x}) d\mathbf{x},$$

where $\tilde{\mathbf{x}}$ is defined as in (2.6),

$$\tilde{\mathbf{x}}^- = \tilde{\mathbf{x}} - \gamma \frac{b(\mathbf{x}, t^n)}{c(\mathbf{x})} (\Delta t^n)^2, \quad \tilde{\mathbf{x}}^+ = \tilde{\mathbf{x}} + \gamma \frac{b(\mathbf{x}, t^n)}{c(\mathbf{x})} (\Delta t^n)^2,$$

and γ is a fixed positive constant (normally chosen to be less than one [17]). If $\tilde{Q}_h^{n-1} = \tilde{Q}_h^{n-1}$, we must accept that mass cannot be conserved; otherwise, find $\Lambda^{n-1} \in \mathbb{R}$ such that

$$Q_h^{n-1} = \Lambda^{n-1} \tilde{Q}_h^{n-1} + (1 - \Lambda^{n-1}) \tilde{Q}_h^{n-1}. \quad (3.4)$$

Define

$$\hat{p}_h^{n-1} = \Lambda^{n-1} \tilde{p}_h^{n-1} + (1 - \Lambda^{n-1}) \tilde{p}_h^{n-1}, \quad (3.5)$$

and

$$\hat{Q}_h^{n-1} = \int_{\Omega} c(\mathbf{x}) \hat{p}_h^{n-1}(\mathbf{x}) d\mathbf{x}.$$

Clearly, $\hat{Q}_h^{n-1} = Q_h^{n-1}$, so the conservation law is preserved. Now, continue in n with \hat{p}_h^{n-1} in place of \tilde{p}_h^{n-1} in the original procedure (2.8); i.e.,

$$\left(c \frac{p_h^n - \hat{p}_h^{n-1}}{\Delta t^n}, v \right) + \sum_{K \in K_h} (a^n \nabla p_h^n, \nabla v)_K + (R^n p_h^n, v) = (f^n, v), \quad \forall v \in V_h. \quad (3.6)$$

Note that Λ^{n-1} is bounded; $0 \leq \Lambda^{n-1} \leq 1$ for small Δt^{n-1} [17]. Theorems 2.1 and 2.2 remain valid here. In addition, the discussion on the examples given in Section 2.3 applies as well.

4. EULERIAN-LAGRANGIAN NONCONFORMING METHODS

The Eulerian-Lagrangian approach is based on the divergence form of (2.1),

$$\begin{aligned} \frac{\partial(cp)}{\partial t} + \nabla \cdot (\mathbf{b}p - \mathbf{a}\nabla p) + Rp &= f, & \mathbf{x} \in \Omega, \quad t > 0, \\ (\mathbf{b}p - \mathbf{a}\nabla p) \cdot \boldsymbol{\nu} &= g, & \mathbf{x} \in \Gamma, \quad t > 0, \\ p(\mathbf{x}, 0) &= p_0(\mathbf{x}), & \mathbf{x} \in \Omega, \end{aligned} \quad (4.1)$$

where $\Omega \subset \mathbb{R}^d$ ($d \leq 3$) is a bounded domain and $\boldsymbol{\nu}$ is the outward unit normal to Γ . For simplicity, we consider a flux boundary condition in (4.1). A Dirichlet or mixed-type condition can be also considered [6].

As in the previous two sections, for any $\mathbf{x} \in \Omega$ and two times $0 \leq t^{n-1} < t^n$, the hyperbolic part of problem (4.1), $c \frac{\partial p}{\partial t} + \mathbf{b} \cdot \nabla p$, defines the characteristic $\tilde{\mathbf{x}}_n(\mathbf{x}, t)$ along the interstitial velocity $\boldsymbol{\varphi} = \mathbf{b}/c$,

$$\begin{aligned} \frac{\partial}{\partial t} \tilde{\mathbf{x}}_n &= \boldsymbol{\varphi}(\tilde{\mathbf{x}}_n, t), & t \in J^n = [t^{n-1}, t^n], \\ \tilde{\mathbf{x}}_n(\mathbf{x}, t^n) &= \mathbf{x}. \end{aligned} \quad (4.2)$$

In general, the characteristics in (4.2) can be determined only approximately. There are many ways to solve this first-order ordinary differential equation for approximate characteristics. We consider only an Euler method, as in the previous two sections.

The Euler method to solve (4.2) for the approximate characteristics is given: for any $\mathbf{x} \in \Omega$, we define

$$\tilde{\mathbf{x}}_n(\mathbf{x}, t) = \mathbf{x} - \boldsymbol{\varphi}(\mathbf{x}, t^n) (t^n - t), \quad t \in [\tilde{t}(\mathbf{x}), t^n], \quad (4.3)$$

where $\tilde{t}(\mathbf{x}) = t^{n-1}$ if $\tilde{\mathbf{x}}_n(\mathbf{x}, t)$ does not backtrack to the boundary Γ for $t \in [t^{n-1}, t^n]$; $\tilde{t}(\mathbf{x}) \in (t^{n-1}, t^n]$ is the time instant when $\tilde{\mathbf{x}}_n(\mathbf{x}, t)$ intersects Γ , i.e., $\tilde{\mathbf{x}}_n(\mathbf{x}, \tilde{t}(\mathbf{x})) \in \Gamma$, otherwise. Let

$$\Gamma_+ = \{\mathbf{x} \in \Gamma : (\mathbf{b} \cdot \boldsymbol{\nu})(\mathbf{x}) \geq 0\}.$$

For $(\mathbf{x}, t) \in \Gamma_+ \times J^n$, the approximate characteristic emanating backward from (\mathbf{x}, t) is given by

$$\tilde{\mathbf{x}}_n(\mathbf{x}, \theta) = \mathbf{x} - \varphi(\mathbf{x}, t)(t - \theta), \quad \theta \in [\tilde{t}(\mathbf{x}, t), t], \quad (4.4)$$

where $\tilde{t}(\mathbf{x}, t) = t^{n-1}$ if $\tilde{\mathbf{x}}_n(\mathbf{x}, \theta)$ does not backtrack to the boundary Γ for $\theta \in [t^{n-1}, t]$; $\tilde{t}(\mathbf{x}, t) \in (t^{n-1}, t]$ is the time instant when $\tilde{\mathbf{x}}_n(\mathbf{x}, \theta)$ intersects Γ otherwise. We have exploited a single step Euler method to determine the approximate characteristics from (4.2); a multistep version can be also employed.

If Δt^n is sufficiently small (depending upon the smoothness of φ), the approximate characteristics do not cross each other, which is assumed. Then $\tilde{\mathbf{x}}_n(\cdot, t)$ is a one-to-one mapping of \mathbb{R}^d to \mathbb{R}^d ($d \leq 3$); we indicate its inverse by $\hat{\mathbf{x}}_n(\cdot, t)$.

For any $t \in (t^{n-1}, t^n]$, we define

$$\tilde{\varphi}(\mathbf{x}, t) = \varphi(\hat{\mathbf{x}}_n(\mathbf{x}, t), t^n), \quad \tilde{\mathbf{b}} = \tilde{\varphi}c. \quad (4.5)$$

We assume that $\tilde{\mathbf{b}} \cdot \boldsymbol{\nu} \geq 0$ on Γ_+ .

Let K_h be a regular partition of Ω into elements $\{K\}$. For each $K \in K_h$, let $\check{K}(t)$ represent the trace-back of K to time t , $t \in J^n$:

$$\check{K}(t) = \{x \in \Omega : \mathbf{x} = \tilde{\mathbf{x}}_n(\mathbf{y}, t) \text{ for some } \mathbf{y} \in K\},$$

and \mathcal{K}^n be the space-time region that follows the characteristics (see Figure 2)

$$\mathcal{K}^n = \{(\mathbf{x}, t) \in \Omega \times J : t \in J^n \text{ and } \mathbf{x} \in \check{K}(t)\}.$$

Also, we define $\mathcal{B}^n = \{(\mathbf{x}, t) \in \partial\mathcal{K}^n : \mathbf{x} \in \Gamma\}$.

We write the hyperbolic part of (4.1) as

$$\frac{\partial(cp)}{\partial t} + \nabla \cdot (\mathbf{b}p) = \frac{\partial(cp)}{\partial t} + \nabla \cdot (\tilde{\mathbf{b}}p) + \nabla \cdot ([\mathbf{b} - \tilde{\mathbf{b}}]p). \quad (4.6)$$

With $\tau(\mathbf{x}, t) = (\tilde{\mathbf{b}}, c)$ and a smooth test function $v(\mathbf{x}, t)$, an application of Green's formula in space and time gives

$$\begin{aligned} \int_{\mathcal{K}^n} \left(\frac{\partial(cp)}{\partial t} + \nabla \cdot (\tilde{\mathbf{b}}p) \right) v \, d\mathbf{x} \, dt &= \int_K c^n p^n v^n \, d\mathbf{x} - \int_{\check{K}(t^{n-1})} c^{n-1} p^{n-1} v^{n-1,+} \, d\mathbf{x} \\ &+ \int_{\mathcal{B}^n} p \tilde{\mathbf{b}} \cdot \boldsymbol{\nu} v \, d\ell - \int_{\mathcal{K}^n} p \boldsymbol{\tau} \cdot \left(\nabla v, \frac{\partial v}{\partial t} \right) \, d\mathbf{x} \, dt, \end{aligned} \quad (4.7)$$

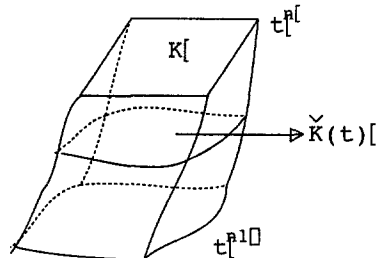


Figure 2. An illustration of \mathcal{K}^n .

where we used the fact that $\boldsymbol{\tau} \cdot \boldsymbol{\nu}_{\mathcal{K}^n} = 0$ on the space-time edges $(\partial\mathcal{K}^n \cap (\tilde{K} \times J^n)) \setminus \mathcal{B}^n$. Similarly, the diffusion part of (4.1) gives

$$\int_{\mathcal{K}^n} \nabla \cdot (\mathbf{a} \nabla p) v \, d\mathbf{x} \, dt = \int_{J^n} \left\{ \int_{\partial\tilde{K}(t)} \mathbf{a} \nabla p \cdot \boldsymbol{\nu}_{\tilde{K}(t)} v \, d\ell - \int_{\tilde{K}(t)} (\mathbf{a} \nabla p) \cdot \nabla v \, d\mathbf{x} \right\} dt. \quad (4.8)$$

We assume that the test function $v(\mathbf{x}, t)$ is constant along the approximate characteristics. Then, combining (4.6)–(4.8), the space-time variational form of (4.1) can be derived as follows:

$$\begin{aligned} & (c^n p^n, v^n) - (c^{n-1} p^{n-1}, v^{n-1,+}) \\ & + \int_{J^n} \{ (\mathbf{a} \nabla p, \nabla v) + (Rp, v) \} \, dt = \int_{J^n} \{ (f, v) - (g, v)_\Gamma \} \, dt \\ & + \int_{J^n} \left\{ \left(\nabla \cdot [(\tilde{\mathbf{b}} - \mathbf{b})p], \hat{v} \right) - \left(p [\tilde{\mathbf{b}} - \mathbf{b}] \cdot \boldsymbol{\nu}, v \right)_\Gamma \right\} dt, \end{aligned} \quad (4.9)$$

where the inner product notation in space is used. If we apply backward Euler time integration along characteristics to the diffusion, reaction, and source term in (4.9), we see that

$$\begin{aligned} & (c^n p^n, v^n) + (\Delta t^n \mathbf{a}^n \nabla p^n, \nabla v^n) + (\Delta t^n R^n p^n, v^n) \\ & = (c^{n-1} p^{n-1}, v^{n-1,+}) + (\Delta t^n f^n, v^n) - \int_{J^n} (g, v)_\Gamma \, dt \\ & + \int_{J^n} \left\{ \left(\nabla \cdot [(\tilde{\mathbf{b}} - \mathbf{b})p], \hat{v} \right) - \left(p [\tilde{\mathbf{b}} - \mathbf{b}] \cdot \boldsymbol{\nu}, v \right)_\Gamma \right\} dt, \end{aligned} \quad (4.10)$$

where $\Delta t^n(\mathbf{x}) = t^n - \tilde{t}(\mathbf{x})$.

Let $V_h \subset H^1(\Omega)$ be a nonconforming finite-element space, as defined in the second section. For any $w \in V_h$, we define a test function $v(\mathbf{x}, t)$ to be a constant extension of $w(\mathbf{x})$ into the space-time region $\Omega \times J^n$ along the approximate characteristics (refer to (4.3) and (4.4)),

$$\begin{aligned} v(\tilde{\mathbf{x}}_n(\mathbf{x}, t), t) &= w(\mathbf{x}), & t \in [\tilde{t}(\mathbf{x}), t^n], & \quad \mathbf{x} \in \Omega, \\ v(\tilde{\mathbf{x}}_n(\mathbf{x}, \theta), \theta) &= w(\mathbf{x}), & \theta \in [\tilde{t}(\mathbf{x}, t), t], & \quad (\mathbf{x}, t) \in \Gamma_+ \times J^n. \end{aligned} \quad (4.11)$$

Now, based on (4.10), the Eulerian-Lagrangian nonconforming method is defined: for $n = 1, 2, \dots$, find $p_h^n \in V_h$ such that

$$\begin{aligned} & (c^n p_h^n, v^n) + \sum_{K \in \mathcal{K}_h} (\Delta t^n \mathbf{a}^n \nabla p_h^n, \nabla v^n) + (\Delta t^n R^n p_h^n, v^n) \\ & = (c^{n-1} p_h^{n-1}, v^{n-1,+}) + (\Delta t^n f^n, v^n) - \int_{J^n} (g, v)_\Gamma \, dt. \end{aligned} \quad (4.12)$$

The discussion of the examples given in Section 2.3 applies to (4.12) as well. In particular, Theorems 2.1 and 2.2 and estimate (2.14) hold. Moreover, estimate (2.15) remains true for the Crouzeix-Raviart and rotated Q_1 elements in two dimensions.

5. THE PROOF OF STABILITY AND CONVERGENCE

In this section, as an example, we carry out the proof of Theorems 2.1 and 2.2 for the MMOC-nonconforming finite-element methods. The same results for the MMOC-AAA and Eulerian-Lagrangian nonconforming methods can be shown by combining the present techniques and those in [7,18] for studying the standard finite-element method.

LEMMA 5.1. *With assumption (2.11), for each n we have*

$$(c\tilde{v}, \tilde{v}) - (cv, v) \leq C\Delta t^n (cv, v), \quad \forall v \in L^2(\Omega),$$

where $\tilde{v}(\mathbf{x}) = v(\mathbf{x} - \mathbf{b}(\mathbf{x}, t^n)\Delta t^n / c(\mathbf{x}))$.

For the proof of this lemma, see [18,19].

PROOF OF THEOREM 2.1. Set $v = p_h^n$ in (2.8), multiply by Δt^n , and sum over n , $1 \leq n \leq N$, to see that

$$\begin{aligned} \sum_{n=1}^N \left\{ (c[p_h^n - \check{p}_h^{n-1}], p_h^n) + \sum_{K \in K_h} (\mathbf{a}^n \nabla p_h^n, \nabla p_h^n)_K \Delta t^n + (R^n p_h^n, p_h^n) \Delta t^n \right\} \\ = \sum_{n=1}^N (f^n, p_h^n) \Delta t^n. \end{aligned} \quad (5.1)$$

Note that

$$\begin{aligned} (c(p_h^n - \check{p}_h^{n-1}), p_h^n) &\geq \frac{1}{2} ((cp_h^n, p_h^n) - (c\check{p}_h^{n-1}, \check{p}_h^{n-1})) \\ &= \frac{1}{2} \{ ((cp_h^n, p_h^n) - (cp_h^{n-1}, p_h^{n-1})) + ((cp_h^{n-1}, p_h^{n-1}) - (c\check{p}_h^{n-1}, \check{p}_h^{n-1})) \}, \end{aligned}$$

so that Theorem 2.1 follows from (5.1), Lemma 5.1, (2.10), and the discrete Gronwall inequality. \blacksquare

LEMMA 5.2. *With assumption (2.11), for each n we have*

$$\|v - \tilde{v}\|_{H^{-1}(\Omega)} \leq K\Delta t^n \|v\|_{L^2(\Omega)}, \quad \forall v \in L^2(\Omega),$$

where $\tilde{v}(\mathbf{x}) = v(\mathbf{x} - \mathbf{b}(\mathbf{x}, t^n)\Delta t^n / c(\mathbf{x}))$.

For the proof of Lemma 5.2, refer to [8].

For the simplicity of the proof of Theorem 2.2, \mathbf{a} is assumed to be independent of t . Also, let V_h be the Crouzeix-Raviart finite-element space as defined in Section 2.3.1. Define

$$A_h(v, w) = \sum_{K \in K_h} (\mathbf{a} \nabla v, \nabla w)_K, \quad v, w \in H^1(\Omega) \cup V_h.$$

We recall (2.5) as

$$\left(\psi \frac{\partial p}{\partial \tau}, v \right) + A_h(p, v) + (Rp, v) = (f, v), \quad \forall v \in V, \quad t > 0. \quad (5.2)$$

We also recall (2.8) as

$$\left(c \frac{p_h^n - \check{p}_h^{n-1}}{\Delta t^n}, v \right) + A_h(p_h^n, v) + (R^n p_h^n, v) = (f^n, v), \quad \forall v \in V_h. \quad (5.3)$$

We define the initial approximation $p_h^0 \in V_h$ by

$$A_h(p_h^0 - p_0, v) = 0, \quad \forall v \in V_h. \quad (5.4)$$

Let $w_h : J \rightarrow V_h$ satisfy

$$A_h(p - w_h, v) = 0, \quad \forall v \in V_h, \quad t \in J. \quad (5.5)$$

Set

$$\eta = p - w_h, \quad \xi = p_h - w_h.$$

It follows from the standard error estimate for the Crouzeix-Raviart element [15] that, for $q = 2$ or ∞ ,

$$\|\eta\|_{L^q(J;L^2(\Omega))} + h\|\eta\|_{L^q(J;H_h^1(\Omega))} \leq Ch^s \|p\|_{L^q(J;H^s(\Omega))}, \quad 1 \leq s \leq 2, \quad (5.6)$$

where $\|\eta\|_{H_h^1(\Omega)}^2 = \sum_{K \in K_h} \|\eta\|_{H^1(K)}^2$. Because the bilinear form $A_h(\cdot, \cdot)$ is independent of time, it also follows that

$$\left\| \frac{\partial \eta}{\partial t} \right\|_{L^2(J;H^{-1}(\Omega))} \leq Ch \left\| \frac{\partial p}{\partial t} \right\|_{L^2(J;H^1(\Omega))}. \quad (5.7)$$

From (5.6) and (5.7), to obtain error bounds for $p - p_h$, it suffices to estimate ξ . For simplicity of exposition, let $\Delta t = \Delta t^n$, $n = 1, 2, \dots, N$.

PROOF OF THEOREM 2.2. Choose $v = \xi^n$ in (5.3) to have

$$\left(c \frac{p_h^n - \tilde{p}_h^{n-1}}{\Delta t^n}, \xi^n \right) + A_h(p_h^n, \xi^n) + (R^n p_h^n, \xi^n) = (f^n, \xi^n), \quad (5.8)$$

and subtract the following quantity from both sides of (5.8):

$$\left(\psi^n \frac{\partial p^n}{\partial \tau}, \xi^n \right) + A_h(p^n, \xi^n) + (R^n p^n, \xi^n)$$

to see that

$$\begin{aligned} \left(c \frac{\xi^n - \tilde{\xi}^{n-1}}{\Delta t}, \xi^n \right) + A_h(\xi^n, \xi^n) &= \left(\psi^n \frac{\partial p^n}{\partial \tau} - c \frac{p^n - \tilde{p}_h^{n-1}}{\Delta t}, \xi^n \right) + \left(c \frac{\eta^n - \tilde{\eta}^{n-1}}{\Delta t}, \xi^n \right) \\ &\quad + (R^n(p^n - p_h^n), \xi^n) + (f^n, \xi^n) - \left(\psi^n \frac{\partial p^n}{\partial \tau}, \xi^n \right) \\ &\quad - A_h(p^n, \xi^n) - (R^n p^n, \xi^n). \end{aligned} \quad (5.9)$$

We need to estimate each term in (5.9).

First, apply a standard backward (in the characteristic direction) difference analysis [8] to have

$$\left| \left(\psi^n \frac{\partial p^n}{\partial \tau} - c \frac{p^n - \tilde{p}_h^{n-1}}{\Delta t}, \xi^n \right) \right| \leq C \left(\Delta t \left\| \frac{\partial^2 p}{\partial \tau^2} \right\|_{L^2(\Omega \times J^n)}^2 + \|\xi^n\|_{L^2(\Omega)}^2 \right). \quad (5.10)$$

Second, we write $\eta^n - \tilde{\eta}^{n-1}$ as the sum of $(\eta^n - \eta^{n-1}) + (\eta^{n-1} - \tilde{\eta}^{n-1})$. Then we see that

$$\begin{aligned} \left| \left(c \frac{\eta^n - \eta^{n-1}}{\Delta t}, \xi^n \right) \right| &\leq \frac{C}{\Delta t} \|\xi^n\|_{H_h^1(\Omega)} \int_{J^n} \left\| \frac{\partial \eta}{\partial t} \right\|_{H^{-1}(\Omega)} dt \\ &\leq \frac{C}{\sqrt{\Delta t}} \|\xi^n\|_{H_h^1(\Omega)} \left(\int_{J^n} \left\| \frac{\partial \eta}{\partial t} \right\|_{H^{-1}(\Omega)}^2 dt \right)^{1/2} \\ &\leq \epsilon \|\xi^n\|_{H_h^1(\Omega)}^2 + \frac{C}{\Delta t} \left\| \frac{\partial \eta}{\partial t} \right\|_{L^2(J^n; H^{-1}(\Omega))}^2, \end{aligned} \quad (5.11)$$

where ϵ is a positive constant, as small as we please. Also, by Lemma 5.2, we have

$$\begin{aligned} \left| \left(c \frac{\eta^{n-1} - \tilde{\eta}^{n-1}}{\Delta t}, \xi^n \right) \right| &\leq C \|\xi^n\|_{H_h^1(\Omega)} \left\| \frac{\eta^{n-1} - \tilde{\eta}^{n-1}}{\Delta t} \right\|_{H^{-1}(\Omega)} \\ &\leq \epsilon \|\xi^n\|_{H_h^1(\Omega)}^2 + C \|\eta^{n-1}\|_{L^2(\Omega)}^2. \end{aligned} \quad (5.12)$$

Third, it is obvious that

$$|(R^n(p^n - p_h^n), \xi^n)| \leq C \left(\|\xi^n\|_{L^2(\Omega)}^2 + \|\eta^n\|_{L^2(\Omega)}^2 \right). \quad (5.13)$$

Fourth, using Green's formula and (2.4), we have

$$(f^n, \xi^n) - \left(\psi^n \frac{\partial p^n}{\partial \tau}, \xi^n \right) - A_h(p^n, \xi^n) - (R^n p^n, \xi^n) = - \sum_{K \in K_h} (\mathbf{a} \nabla p^n \cdot \boldsymbol{\nu}, \xi^n)_{\partial K},$$

where $\boldsymbol{\nu}$ is the outward unit normal to ∂K , so that, by a scaling argument [15],

$$\left| (f^n, \xi^n) - \left(\psi^n \frac{\partial p^n}{\partial \tau}, \xi^n \right) - A_h(p^n, \xi^n) - (R^n p^n, \xi^n) \right| \leq Ch |p^n|_{H^2(\Omega)} \|\xi^n\|_{H_h^1(\Omega)}. \quad (5.14)$$

This completes the treatment of the right-hand side of (5.9).

The left-hand side is bounded below:

$$\begin{aligned} \left(c \frac{\xi^n - \check{\xi}^{n-1}}{\Delta t}, \xi^n \right) + A_h(\xi^n, \xi^n) &\geq \frac{1}{2\Delta t} [(c\xi^n, \xi^n) - (c\check{\xi}^{n-1}, \check{\xi}^{n-1})] + A_h(\xi^n, \xi^n) \\ &= \frac{1}{2\Delta t} [(c\xi^n, \xi^n) - (c\check{\xi}^{n-1}, \xi^{n-1}) (1 + \gamma^n C \Delta t)] \\ &\quad + A(\xi^n, \xi^n), \quad |\gamma^n| \leq 1. \end{aligned} \quad (5.15)$$

Inequalities (5.10)–(5.15) can be combined with (5.9) to give the recursion relation

$$\begin{aligned} &\frac{1}{2\Delta t} [(c\xi^n, \xi^n) - (c\check{\xi}^{n-1}, \xi^{n-1})] + \frac{a_*}{2} \|\xi^n\|_{H_h^1(\Omega)}^2 \\ &\leq C \left\{ \|\xi^n\|_{L^2(\Omega)}^2 + \|\xi^{n-1}\|_{L^2(\Omega)}^2 + h^2 |p^n|_{H^2(\Omega)}^2 + \Delta t \left\| \frac{\partial^2 p}{\partial \tau^2} \right\|_{L^2(\Omega \times J^n)}^2 \right. \\ &\quad \left. + \frac{1}{\Delta t} \left\| \frac{\partial \eta}{\partial t} \right\|_{L^2(J^n; H^{-1}(\Omega))}^2 + \|\eta^{n-1}\|_{L^2(\Omega)}^2 + \|\eta^n\|_{L^2(\Omega)}^2 \right\}. \end{aligned} \quad (5.16)$$

It follows from (5.3) that $\xi^0 = 0$. If we multiply (5.16) by $2\Delta t$, sum over n , and apply the discrete Gronwall inequality, it follows that

$$\begin{aligned} \max_{1 \leq n \leq N} \|\xi^n\|_{L^2(\Omega)} + \left(\sum_{n=1}^N \|\xi^n\|_{H_h^1(\Omega)}^2 \Delta t \right)^{1/2} &\leq C \left\{ h \|p\|_{L^\infty(J; H^2(\Omega))} + \Delta t \left\| \frac{\partial^2 p}{\partial \tau^2} \right\|_{L^2(\Omega_T)} \right. \\ &\quad \left. + \left\| \frac{\partial \eta}{\partial t} \right\|_{L^2(J; H^{-1}(\Omega))} + \|\eta\|_{L^\infty(J; L^2(\Omega))} \right\}, \end{aligned}$$

which, together with (5.6) and (5.7), yields the desired result. \blacksquare

REFERENCES

1. J.W. Barrett and K.W. Morton, Approximate symmetrization and Petrov-Galerkin methods for diffusion-convection problems, *Comp. Mech. Appl. Mech. Engrg.* **45**, 97–122, (1984).
2. A. Brooks and T.J. Hughes, Streamline upwind Petrov-Galerkin formulations for convection dominated flows with particular emphasis on the incompressible Navier-Stokes equations, *Comp. Mech. Appl. Mech. Engrg.* **32**, 199–259, (1982).
3. I. Christie, D.F. Griffiths and A.R. Mitchell, Finite element methods for second order differential equations with significant first derivatives, *Int. J. Num. Engrg.* **10**, 1389–1396, (1976).
4. J.J. Westerink and D. Shea, Consistent higher degree Petrov-Galerkin methods for the solution of the transient convection-diffusion equation, *Int. J. Num. Meth. Engrg.* **13**, 839–941, (1989).

5. T. Arbogast and M.F. Wheeler, A characteristics-mixed finite element for advection-dominated transport problems, *SIAM J. Numer. Anal.* **32**, 404–424, (1995).
6. M.A. Celia, T.F. Russell, I. Herrera and R.E. Ewing, An Eulerian Lagrangian localized adjoint method for the advection-diffusion equation, *Advances in Water Resources* **13**, 187–206, (1990).
7. Z. Chen, Characteristic mixed discontinuous finite element methods for advection-dominated diffusion problems, *Comp. Meth. Appl. Mech. Engrg.* **191**, 2509–2538, (2002).
8. J. Douglas, Jr. and T.F. Russell, Numerical methods for convection dominated diffusion problems based on combining the method of characteristics with finite element or finite difference procedures, *SIAM J. Numer. Anal.* **19**, 871–885, (1982).
9. O. Pironneau, On the transport-diffusion algorithm and its application to the Navier-Stokes equations, *Numer. Math.* **38**, 309–332, (1982).
10. M. Crouzeix and P. Raviart, Conforming and nonconforming finite element methods for solving the stationary Stokes equations, *RAIRO* **3**, 33–75, (1973).
11. P. Oswald, On a hierarchical basis multilevel method with nonconforming P1 elements, *Numer. Math.* **62**, 189–212, (1992).
12. Z. Chen, Projection finite element methods for semiconductor device equations, *Computers Math. Applic.* **25**, 81–88, (1993).
13. R. Rannacher and S. Turek, Simple nonconforming quadrilateral Stokes element, *Numer. Meth. Partial Diff. Equations* **8**, 97–111, (1992).
14. Z. Chen and P. Oswald, Multigrid and multilevel methods for nonconforming rotated Q1 elements, *Math. Comp.* **67**, 667–693, (1998).
15. P.G. Ciarlet, *The Finite Element Method for Elliptic Problems*, North-Holland, Amsterdam, (1978).
16. T. Arbogast and Z. Chen, On the implementation of mixed methods as nonconforming methods for second order elliptic problems, *Math. Comp.* **64**, 943–972, (1995).
17. J. Douglas, Jr., F. Furtado and F. Pereira, On the numerical simulation of water flooding of heterogeneous petroleum reservoirs, *Computational Geosciences* **1**, 155–190, (1997).
18. Z. Chen, R.E. Ewing, E.Q. Jiang and A.M. Spagnuolo, Error analysis for characteristics-based methods for degenerate parabolic problems, *SIAM J. Numer. Anal.* **40**, 1491–1515, (2002).
19. C.N. Dawson, T.F. Russell and M.F. Wheeler, Some improved error estimates for the modified method of characteristics, *SIAM J. Numer. Anal.* **26**, 1487–1512, (1989).